

Last modified January 22, 2018

Evolution of the Cluster Correlation Function

Neta A. Bahcall¹, Lei Hao¹, Paul Bode¹, Feng Dong¹

ABSTRACT

We study the evolution of the cluster correlation function and its richness-dependence from $z = 0$ to $z = 3$ using large-scale cosmological simulations. A standard flat Λ CDM model with $\Omega_m = 0.3$ and, for comparison, a tilted $\Omega_m = 1$ model, TSCDM, are used. The evolutionary predictions are presented in a format suitable for direct comparisons with observations. We find that the cluster correlation strength increases with redshift: high redshift clusters are clustered more strongly (in comoving scale) than low redshift clusters of the same mass. The increased correlations with redshift, in spite of the decreasing mass correlation strength, is caused by the strong increase in cluster bias with redshift: clusters represent higher density peaks of the mass distribution as the redshift increases. The richness-dependent cluster correlation function, presented as the correlation-scale versus cluster mean separation relation, $R_0 - d$, is found to be, remarkably, independent of redshift to $z \lesssim 2$ for Λ CDM and $z \lesssim 1$ for TSCDM (for a fixed correlation function slope and cluster mass within a fixed comoving radius). The non-evolving $R_0 - d$ relation implies that both the comoving clustering scale and the cluster mean separation increase with redshift for the same mass clusters so that the $R_0 - d$ relation remains essentially unchanged. For Λ CDM, this relation is $R_0(z) \simeq 2.6\sqrt{d(z)}$ for $z \lesssim 2$ (in comoving h^{-1} Mpc scales). TSCDM has smaller correlation scales, as expected. Evolution in the relation is seen at $z \gtrsim 2$ for Λ CDM and $z \gtrsim 1$ for TSCDM, where the amplitude of the relations declines. The evolution of the $R_0 - d$ relation from $z \sim 0$ to $z \sim 3$ provides an important new tool in cosmology; it can be used to break degeneracies that exist at $z \sim 0$ and provide precise determination of cosmological parameters.

Subject headings: cosmology:observations–cosmology:theory–cosmological parameters–dark matter–galaxies:clusters: general–large-scale structure of universe

¹Princeton University Observatory, Princeton, NJ 08544

1. Introduction

The correlation function of clusters of galaxies provides a powerful test of cosmological models: both the amplitude of the correlation function and its dependence on cluster mass/richness are determined by the underlying cosmology. It has long been shown that clusters are more strongly correlated in space than galaxies – by an order-of-magnitude: the typical galaxy correlation scale of $\sim 5 h^{-1}$ Mpc increases to $\sim 20 - 25 h^{-1}$ Mpc for the richest clusters (Bahcall & Soneira 1983; Klypin & Kopylov 1983, see also Bahcall 1988; Huchra et al. 1990; Postman, Huchra, & Geller 1992; Bahcall & West 1992; Peacock & West 1992; Dalton et al. 1994; Croft et al. 1997; Abadi, Lambas, & Muriel 1998; Lee & Park 1999; Borgani, Plionis, & Kolokotronis 1999; Collins et al. 2000; Gonzalez, Zaritsky, & Wechsler 2002; Bahcall et al. 2003c; and references therein). Bahcall & Soneira (1983) showed that the cluster correlation function is richness dependent: the correlation strength increases with cluster richness, or mass. The rarest, most massive clusters exhibit the strongest spatial correlations. Many observations have since confirmed these results (see references above), and theory has nicely explained them (Kaiser 1984; Bahcall & Cen 1992; Mo & White 1996; Governato et al. 1999; Colberg et al. 2000; Moscardini et al. 2001; Bahcall et al. 2003c; and references therein). All analyses so far have been done at small redshifts, $z \lesssim 0.5$. As cluster samples become available at larger redshifts, it is important to determine the expected evolution of the cluster correlation function and the evolution of its richness dependence as a function of redshift; these will provide direct cosmological predictions for comparisons with the data. Analytic approximations for the evolution of cluster halo abundance, bias and clustering have been presented by several groups (Mann, Heavens & Peacock 1993; Mo & White 1996, 2002; Sheth, Mo, & Tormen 2001; Moscardini et al. 2001). Here we use direct N-body cosmological simulations to determine the expected evolution of the cluster correlation function and present the results in a format suitable for direct comparison with observations.

We use large-scale high-resolution cosmological simulations to investigate the evolution of the cluster correlation function from $z = 0$ to $z = 3$ over a wide range of cluster masses. We determine the evolution of the richness dependence of the cluster correlation function over the same redshift range. The simulations use a standard flat LCDM model which best fits numerous other observations (e.g., Bahcall, Ostriker, Perlmutter, & Steinhardt 1999; Bennett et al. 2003; Spergel et al. 2003). For comparison, we also investigate the evolution of the cluster correlation function in an $\Omega_m = 1$ tilted SCDM model.

2. Simulations

The high-resolution N-body simulations use a standard flat Lambda CDM cosmology with $\Omega_m = 0.3$, $h = 0.67$, $n = 1$, and $\sigma_8 = 0.9$. For comparison, we also investigate an $\Omega_m = 1$ Tilted SCDM model (TSCDM; with $h = 0.5$, $\sigma_8 = 0.5$, $n = 0.625$). The simulations are discussed in detail by Bode et al. (2000, 2001). A brief summary is given below.

The simulations employ $512^3 = 1.34 \times 10^8$ particles in a periodic cube, with a particle mass of $6.2 \times 10^{11} h^{-1} M_\odot$. A larger simulation with 1024^3 particles and one eighth the particle mass was also investigated for comparison; it yields consistent results. The box length is $1000 h^{-1}$ Mpc for the LCDM model ($669.4 h^{-1}$ Mpc for TSCDM). The spline kernel softening length is $27 h^{-1}$ kpc. The spatial resolution is comfortably smaller than the typical ~ 100 kpc core size of clusters. The N-body evolution was carried out with the tree-particle-mesh (TPM) code (Bode et al. 2000; Bode & Ostriker 2003). These are among the largest volume simulations currently available.

Clusters were selected in the simulations using the HOP algorithm for the detection of high-density peaks (Eisenstein & Hut 1998) as described in Bode et al. (2001). Cluster masses are defined within a comoving radius of $1.5 h^{-1}$ Mpc of the cluster center. Cluster masses within other fixed radii yield similar results. Clusters with mass threshold of $M_{1.5} \geq 2 \times 10^{13} h^{-1} M_\odot$ (within comoving radius $1.5 h^{-1}$ Mpc) are selected at redshifts $z = 0, 0.17, 0.5, 1, 2$, and 3 . The number of clusters used ranges from 2×10^5 clusters (for $z = 0$, $M_{1.5} \geq 2 \times 10^{13} M_\odot$) to $\sim 10^3$ clusters for the highest mass, highest redshift clusters. The abundance of LCDM clusters (2×10^{-4} and $1.4 \times 10^{-5} h^3 \text{ Mpc}^{-3}$ for $M_{1.5} \geq 2 \times 10^{13}$ and $2 \times 10^{14} h^{-1} M_\odot$ at $z = 0$) is consistent with recent observations of SDSS and X-ray clusters (Bahcall et al. 2003a; Ikebe et al. 2002; Reiprich & Bohringer 2002). For more details see Bode et al. (2001).

3. Evolution of the Cluster Correlation Function

We determine the two-point spatial correlation function of clusters at different redshifts as a function of cluster mass threshold. The comoving mass thresholds range from $M_{1.5} \geq 2 \times 10^{13} h^{-1} M_\odot$ (within $1.5 h^{-1}$ comoving Mpc) to $5 \times 10^{14} h^{-1} M_\odot$. The redshifts investigated range from $z = 0$ to 3 . The correlation function is determined for each sample by comparing the observed distribution of cluster pairs as a function of pair separation with the distribution in random catalogs within the same volume: $\xi_{cc}(r) = F_{DD}(r)/F_{RR}(r) - 1$, where $F_{DD}(r)$ and $F_{RR}(r)$ are the frequencies of cluster-cluster pairs as a function of pair separation r in the data and in random catalogs, respectively. The number of clusters decreases with increasing

mass and redshift, from 2×10^5 to $\sim 10^3$ clusters; the most massive (rarest) clusters are therefore studied only at the lower part of the redshift range. Since the cluster abundance in a TSCDM model decreases more rapidly with redshift than in LCDM, this model is only studied up to $z = 1$. Poisson statistical error-bars are used in the correlation function analysis. Comoving scales and a Hubble constant of $H_0 = 100 \ h \ km \ s^{-1} \ Mpc^{-1}$ are used throughout.

The evolution of the cluster correlation function as a function of redshift is illustrated in Figure 1 for LCDM for two mass threshold samples (2×10^{13} and $1 \times 10^{14} \ h^{-1} \ M_\odot$). The best-fit power-law correlation function, $\xi(r) = (\frac{r}{R_0})^{-\gamma}$, is also presented for each sample. The best fits are derived for scales $r \leq 50 \ h^{-1} \ Mpc$. The power-law slope was treated both as a free parameter and as a fixed value of $\gamma = 2$; the latter is the typical slope found in the simulations. The best-fits shown in Figure 1 are for a fixed slope $\gamma = 2$. The results are similar for a free slope fit, as discussed below. The evolution of the cluster correlation function is apparent in Figure 1: clusters are more strongly correlated at higher redshift. This is of course opposite to the evolution of the mass correlation function, which decreases with redshift. The enhancement of the cluster correlation strength with redshift is due to the increased bias of the clusters relative to the underlying mass distribution: i.e., the same comoving mass clusters represent higher density peaks of the mass distribution as the redshift increases thus amplifying their correlation strength (see, for example, Cole & Kaiser 1989; Mo & White 1996, 2002; Sheth, Mo, & Tormen 2001; Moscardini et al. 2001)

Figure 2 presents the best-fit correlation function slope γ as a function of cluster redshift and cluster mass. The best slope for LCDM is $\gamma \sim 2$ for $z \lesssim 0.5$ clusters. The slope steepens by $\sim 20\%$, to $\gamma \sim 2.3 - 2.5$, as the redshift increases to $z \sim 2 - 3$. This steepening can also be seen in the correlation function of the high-redshift samples in Figure 1. The TSCDM model (Figure 2b) yields a slightly steeper average slope: ~ 2.3 at $z \lesssim 0.5$, increasing only slightly to ~ 2.5 at $z \sim 1$.

The evolution of the cluster correlation function is presented in Figure 3 for clusters with different mass thresholds. The figure illustrates the dependence of the comoving correlation scale, R_0 , on redshift. The results are shown for a correlation slope of 2 as well as for a free fit slope. As expected, the slight steepening of the best-fit slope at high redshift causes the correlation scale at high redshift to be somewhat smaller than for $\gamma = 2$. The changing slope does not change the main evolutionary trend of $R_0(z)$. Two main results are apparent in Figure 3: a) the cluster correlation scale increases with redshift; b) the evolutionary increase of the correlation scale is stronger for the more massive clusters as well as at higher redshifts; low mass and low redshift clusters show only a small increase of R_0 with z . For example, the low mass sample with $M_{1.5} \geq 2 \times 10^{13} \ M_\odot$ increases its correlation scale from $\sim 10 \ h^{-1} \ Mpc$

at $z = 0$ to $11 h^{-1}$ Mpc at $z = 1$ and $18 h^{-1}$ Mpc at $z = 3$ (for LCDM), while $M_{1.5} \geq 2 \times 10^{14} M_{\odot}$ clusters increase their R_0 from $\sim 16 h^{-1}$ Mpc at $z = 0$ to $25 h^{-1}$ Mpc at $z = 1$. The TSCDM model (Figure 3b) shows a similar (but faster) increase of R_0 with z . As expected, the R_0 values of the TSCDM model are smaller than those of LCDM (at low redshift). The observed increase of the correlation scale with cluster mass threshold seen in Figure 3 is the well-known richness-dependence of the cluster correlation function (Bahcall & Soneira 1983; Peacock & West 1992; Bahcall & West 1992; Mo & White 1996, 2002; Governato et al. 1999; Collins et al. 2000; Bahcall et al. 2003c). The strengthening of the cluster correlations with redshift implies that the cluster bias increases with redshift more strongly than the mass correlations decrease with redshift.

4. Evolution of the $R_0 - d$ Relation

The cluster correlation strength increases with both cluster mass and cluster redshift. Here we combine the two by investigating the evolution of the richness-dependent cluster correlation function. We present the richness-dependent correlation function as the dependence of the correlation scale R_0 on the cluster mean separation d (Bahcall & Soneira 1983; Szalay & Schramm 1985; Bahcall 1988; Croft et al. 1997; Governato et al. 1999; Colberg et al. 2000; Bahcall et al. 2003c; and references therein). Samples with intrinsically larger mean separation correspond to lower intrinsic cluster abundance ($n_{cl} = d^{-3}$) and thus to higher cluster richness and mass (for complete samples). Since the cluster mass does not enter this relation, the predictions can be easily compared with observations.

In Figure 4 we present the $R_0 - d$ relation for different redshifts for the LCDM and TSCDM models. A fixed correlation function slope of $\gamma = 2$ is used. Remarkably, the richness-dependent correlation function, $R_0 - d$, is independent of redshift for $z \lesssim 2$ for LCDM and $z \lesssim 1$ for TSCDM. The scatter in the $R_0 - d$ relation with redshift is small when a fixed slope ($\gamma = 2$) is used in determining R_0 . For a free fit slope (LCDM; Figure 5), the correlation scales at high redshift are slightly lower due to the steepening of the slope γ at high z . This results in a small amount of evolution in the $R_0 - d$ relation for $d \gtrsim 50 h^{-1}$ Mpc, where the amplitude of the relation decreases by $\lesssim 10\%$ as the redshift increases from $z = 0$ to $z = 2$ (Figure 5; to $d \sim 100 h^{-1}$ Mpc). The $R_0 - d$ relation for the TSCDM model remains essentially un-evolving for $z < 1$ for both fixed and free slopes (Figure 5). The best-fit slope for this model changes only slightly with redshift (Figure 2). Using a slope of 2.3 instead of 2 makes only a small difference in the $R_0 - d$ relation (Figure 3). The $R_0 - d$ relation evolves at $z \gtrsim 2$ for LCDM ($\gamma = 2$), where the amplitude of the relation declines. The same is suggested for TSCDM at $z \gtrsim 1$. The above results use cluster masses defined within a

fixed comoving radius ($1.5 h^{-1}$ Mpc); these masses are observationally easy to determine. Using cluster virial masses (or Friend-of-Friend masses to a given mass-density threshold), which are observationally more difficult to determine, yield similar results but with slightly more evolution at large d 's ($\lesssim 10\%$ decrease in the $R_0 - d$ amplitude as the redshift increases from $z = 0$ to 2 for LCDM with $\gamma = 2$, and $\lesssim 15\%$ decrease for a free-fit slope). Only little evolution is seen for $z \lesssim 1$ ($< 10\%$). In addition, the amplitude of the $R_0 - d$ relation is slightly lower ($\lesssim 10\%$) at small separations ($d \lesssim 40 h^{-1}$ Mpc) for these masses, but with no significant evolution to $z \lesssim 1$. An analysis of the clustering in $\Omega_m = 1$ mixed dark matter models (Gardini et al. 2000) similarly yields an $R_0 - d$ relation that is essentially the same at $z = 0$ and $z = 0.8$. The results presented here, for cluster masses within a fixed comoving radius, can be directly compared with observations; the latter are to be defined in a similar manner.

A higher resolution LCDM simulation with 1024^3 particles yields consistent results (within 5% for $d \lesssim 60 h^{-1}$ Mpc and 10% ($\sim 2\text{-}\sigma$ level) for $d > 60 h^{-1}$ Mpc) with those presented in Figures 4 and 5.

The remarkable constancy of the $R_0 - d$ relation to these high redshifts, with no significant evolution, implies that the increased cluster correlation strength with redshift (Figure 3) is matched by the increased mean separation d (i.e., lower cluster abundance) so that the $R_0 - d$ relation remains essentially unchanged. For a given mass cluster, the cluster abundance decreases with redshift; the decrease is rapid for low σ_8 models and slow for high σ_8 models (e.g., Bahcall & Fan 1998); the cluster mean separation d therefore increases with redshift, as expected. The evolution of the cluster correlation scale R_0 depends on the combined evolution of the underlying mass correlation function (which decreases with increasing redshift: the decrease is rapid for $\Omega_m = 1$ models and slower for low Ω_m models), and the evolution of the cluster bias relative to the underlying mass distribution. The cluster bias increases with redshift: the same mass clusters represent higher density peaks at high redshift. The bias increases more rapidly for high Ω_m models than for lower Ω_m models (see, e.g., Cole & Kaiser 1989; Mo & White 1996, 2002; Sheth, Mo, & Tormen 2001). The combined effect of the decreasing mass correlation strength and the increasing cluster bias with redshift (for same mass clusters) results in an increasing cluster correlation scale with redshift as seen in Figure 3. The increased $R_0(z)$ matches the increase in the mean separation $d(z)$ in the relative $R_0 - d$ relation (for $\gamma = 2$). Since $R_0 \sim d^{0.5}$ (see below), $R_0(z)$ increases roughly as $d(z)^{0.5}$. The same mass clusters therefore shift upwards along the $R_0 - d$ relation, to larger d and larger R_0 , as the redshift increases. At some high redshift ($z \sim 2$ for LCDM; $z \sim 1$ for TSCDM) the drop in cluster abundance (increase in d) becomes considerably stronger than the increase in clustering scale R_0 , and the amplitude of the $R_0 - d$ relation declines as seen in Figure 4. The results are not sensitive to the precise value of σ_8 ; the $R_0 - d$ relation

changes by $\lesssim 10\%$ at low redshifts as σ_8 changes from 0.9 to 0.7 (values within this range are suggested by recent observations; see, e.g., Ikebe et al. 2002; Reiprich & Bohringer 2002; Bahcall et al. 2003a; Pierpaoli et al. 2003; Schuecker et al. 2003; Spergel et al. 2003; Tegmark et al. 2003). The redshift at which evolution in the $R_0 - d$ relation becomes significant is expected to depend on σ_8 ; the detailed dependance needs to be investigated by simulations.

The evolution of the $R_0 - d$ relation provides an important cosmological tool. The results can be used for direct comparison with observations at any redshift ($z \lesssim 3$). No significant evolution in the $R_0 - d$ relation is expected to $z \lesssim 2$ (using $\gamma = 2$ and cluster mass within fixed comoving radius) if the current LCDM model is correct. An approximation for the $R_0 - d$ relation for LCDM is given by (see Bahcall et al. 2003c):

$$R_0(z) \simeq 2.6 \times d(z)^{0.5} \quad (LCDM; \quad z \lesssim 2; \quad \gamma = 2; \quad d \simeq 20 - 100) \quad (1)$$

where all scales are in comoving h^{-1} Mpc. This approximation holds for all $z \lesssim 2$ clusters (using a slope $\gamma = 2$ and cluster mass within fixed comoving radius) in the range $d \sim 20 - 100h^{-1}$ Mpc. As cluster samples become available at high redshift, this comparison should provide an important test of the LCDM cosmology.

Observations of the cluster correlation function at $z \sim 0$ have been influential in cosmology; they provided some of the earliest evidence that contradicted the then standard $\Omega_m = 1$ model and indicated a low-density universe (e.g. White et al. 1997; Bahcall 1988; Bahcall & Cen 1992). But the $z \sim 0$ data are insufficient by themselves to place a precise constraint on the cosmological parameters. This is so not only because of the observational scatter among different samples, but mainly because the $z \sim 0$ relation is degenerate with respect to different cosmological parameters. For example, the amplitude of the $R_0 - d$ relation at $z \sim 0$ increases with increasing σ_8 but it also increases with decreasing Ω_m ; models with higher σ_8 and higher Ω_m yield degenerate results with models of lower σ_8 and lower Ω_m . The slope of the power-spectrum of mass fluctuation introduces yet another free parameter in the degeneracy. This degeneracy can be broken by studying the evolution of the $R_0 - d$ relation to high redshifts, since the evolution depends differently on the combination of the cosmological parameters. While other independent observations can also be used – such as the cluster mass function and its evolution, and the CMB spectrum of fluctuations – the $R_0 - d(z)$ evolution provides an independent consistency test that uses a single self-consistent method of cluster correlations.

5. Conclusions

We use large-scale high-resolution cosmological simulations to determine the evolution of the cluster correlation function with redshift from $z = 0$ to $z = 3$ over a wide range of cluster masses. Two cosmological models are studied: the standard flat LCDM model (with $\Omega_m = 0.3$), which best fits numerous observations, and, for comparison, a tilted $\Omega_m = 1$ model (TSCDM). The evolutionary predictions are presented in a format suitable for direct comparisons with observations.

We find that the cluster correlation strength increases with redshift for fixed mass clusters; i.e., clusters are more strongly clustered in space at high redshift. The evolutionary increase of the correlation scale with redshift (in comoving units) is faster for more massive clusters and at higher redshift. The increased clustering of clusters at high redshift, in spite of the decreased clustering of the underlying mass distribution, is due to the strongly increasing bias of clusters at high redshift: clusters represent higher-density peaks of the mass distribution at higher redshift. The increased bias dominates over the decreasing mass correlations and causes the clustering of clusters to increase.

We combine the evolution of the cluster correlation function with its dependence on cluster mass by determining the evolution of the richness-dependent cluster correlation function. We do so using the format of the correlation scale versus mean separation relation, $R_0 - d$. This relation is easy to compare with observations. Samples with intrinsically larger mean separations correspond to lower intrinsic cluster abundances and thus to higher cluster richness and mass (for complete samples). We find that, remarkably, the richness-dependent cluster correlation function $R_0 - d$ is independent of redshift for these models for $z \lesssim 2$ for LCDM (using a fixed correlation function slope and cluster mass defined within a fixed comoving radius) and $z \lesssim 1$ for TSCDM (Figure 4). The amplitude of the $R_0 - d$ relation begins to decline only at $z \gtrsim 2$ for LCDM and $z \gtrsim 1$ for TSCDM. Using a free correlation slope fit, or virial cluster masses, yields similar results but with a small amount of evolution ($\lesssim 15\%$ to $z \lesssim 2$ for LCDM).

The non-evolving $R_0 - d$ relation implies that the strengthening of the cluster correlation function with redshift is matched by the relevant increase in the mean separation at high redshift (lower cluster abundance). The same mass clusters shift upwards along the $R_0 - d$ relation as the redshift increases: both the comoving clustering scale and the cluster mean separation increase with redshift so that the $R_0 - d$ relation remains essentially unchanged. At $z \lesssim 2$, the LCDM relation follows approximately $R_0(z) \simeq 2.6\sqrt{d(z)}$ (comoving scales).

The evolution of the $R_0 - d$ relation to high redshift provides an important new cosmological tool. The observed evolution of the relation from $z \simeq 0$ to $z \sim 3$ can be used to

break degeneracies that exist at $z \sim 0$ and thus allow a precise determination of cosmological parameters. No evolution in the $R_0 - d$ relation is expected (using a correlation slope $\gamma = 2$) for $z \lesssim 2$ if the current LCDM model is correct.

REFERENCES

- Abadi, M., Lambas, D., & Muriel, H. 1998, ApJ, 507, 526
- Bahcall, N. A. & Soneira, R. M. 1983, ApJ, 270, 20
- Bahcall, N. A. 1988, ARA&A, 26, 631
- Bahcall, N. A. & West, M. J. 1992, ApJ, 392, 419
- Bahcall, N. A. & Cen, R. 1992, ApJ, 398, L81
- Bahcall, N. A. & Fan, X. 1998, ApJ, 504, 1
- Bahcall, N. A., Ostriker, J. P., Perlmutter, S., & Steinhardt, P. J. 1999, Science, 284, 1481
- Bahcall, N. A., Dong, F., Bode, P. et al. 2003a, ApJ, 585, 182
- Bahcall, N. A. et al. 2003b, ApJS, vol.148 (October 2003), astro-ph/0305202
- Bahcall, N. A., Dong, F., Hao, L., Bode, P., Annis, J., Gunn, J. E., & Schneider, D. P. 2003c, submitted to ApJL, astro-ph/0307102
- Bennett, C. L. et al. 2003, ApJS, 148, 1
- Bode, P., Ostriker, J. P., Xu, G. 2000, ApJS, 128, 561
- Bode, P., Bahcall, N. A., Ford, E. B., & Ostriker, J. P., 2001, ApJ, 551, 15
- Bode, P. & Ostriker, J. P., 2003, ApJS, 145, 1
- Borgani, S., Plionis, M., & Kolokotronis, V. 1999, MNRAS, 305, 866
- Colberg, J. M. et al. 2000, MNRAS, 319, 209
- Cole, S. & Kaiser, N. 1989, MNRAS, 237, 1127
- Collins, C. et al. 2000, MNRAS, 319, 939
- Croft, R. A. C. et al. 1997, MNRAS, 291, 305

- Dalton, G. B. et al. 1994, MNRAS, 271, L47
- Eisenstein, D. J. & Hut, P. 1998, ApJ, 498, 137
- Evrard, A. E. 1998, in *Evolution of Large Scale Structure: From Recombination to Garching*, ed. A. J. Banday, R. K. Sheth, & L. N. da Costa (Enschede: PrintPartners Ipskamp), 249
- Gardini, A., Bonometto, S. A., Murante, G., & Yepes, G., 2000, ApJ, 542, 9
- Gonzalez, A. H., Zaritsky, D., Wechsler, R. H. 2002, ApJ, 571, 129
- Governato, F. et al. 1999, MNRAS, 307, 949
- Huchra, J., Henry, J. P., Postman, M., & Geller, M. 1990, ApJ, 365, 66
- Ikebe, Y., Reiprich, T. H., Bohringer, H., Tanaka, Y. & Kitayama, T. 2002, A&A, 383, 773
- Jenkins, A., Frenk, C. S., White, S. D. M., Colberg, J. M., Cole, S., Evrard, A. E., & Yoshida, N. 2001, MNRAS, 321, 372
- Kaiser, N. 1984, ApJ, 284, L9
- Klypin, A. A. & Kopylov, A. I. 1983, Soviet Astron. Lett. 9, 41
- Lee, S., Park, C. 1999, JKAS, 32, 1
- Mann, R. G., Heavens, A. F., Peacock, J. A. 1993, MNRAS, 263, 798
- Mo, H. J. & White, S. D. M. 1996, MNRAS, 282, 347
- Mo, H. J. & White, S. D. M. 2002, MNRAS, 336, 112
- Moscardini, L., Matarrese, S., Lucchin, F., Rosati, P. 2000, MNRAS, 316, 283
- Moscardini, L., Matarrese, S., Mo, H. J. 2001, MNRAS, 327, 422
- Nichol, R. C., Collins, C. A., Guzzo, L., & Lumsden, S. L. 1992, MNRAS, 255, 21
- Peacock, J. A. & West, M. J. 1992, MNRAS, 259, 494
- Pierpaoli, E., Borgani, S., Scott, D., & White, M. 2003, MNRAS, 342, 163
- Postman, M., Huchra, J., & Geller, M. 1992, ApJ, 384, 404
- Reiprich, T. H., & Bohringer, H. 2002, ApJ, 567, 716

- Schuecker, P., Bohringer, H., Collins, C. A., & Guzzo, L. 2003, *A&A*, 402, 53
- Sheth, R. K., Mo, H. J., Tormen, G. 2001, *MNRAS*, 323, 1
- Smith, J. A. et al. 2002, *AJ*, 123, 2121
- Spergel, D. N. et al. 2003, *ApJS*, 148, 175
- Szalay, A. S. & Schramm, D. N. 1985, *Nature*, 314, 718
- Tegmark, M. et al 2003, in preparation
- White, S. D. M. et al. 1987, *ApJ*, 313, 505

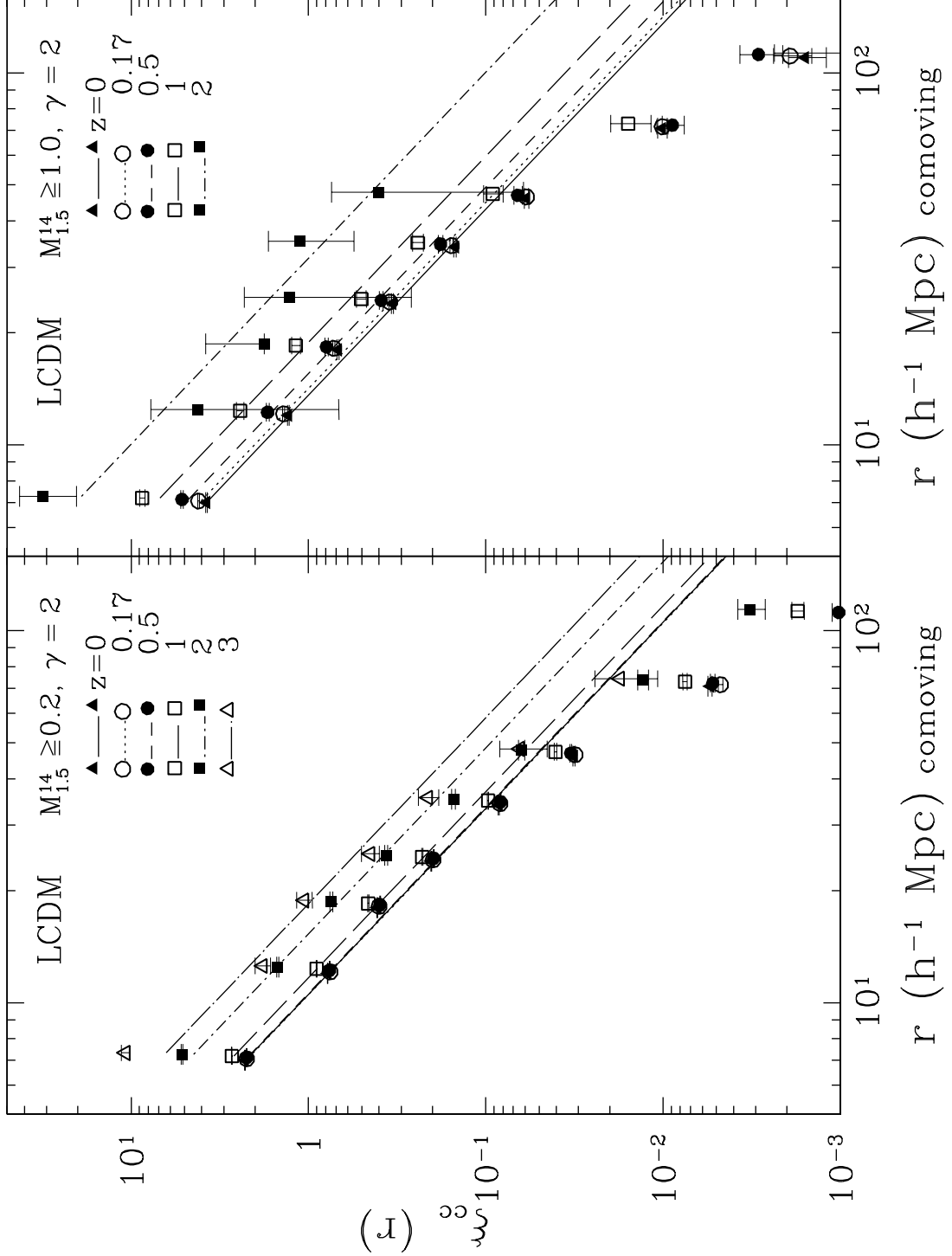


Fig. 1.— The cluster correlation functions at different redshifts, from $z = 0$ to $z = 3$, for two mass threshold samples ($M(r \leq 1.5 h^{-1} \text{ Mpc comoving}) \geq 0.2 \times 10^{14}$ and $1 \times 10^{14} h^{-1} M_{\odot}$), for the LCDM model. The lines are the best-fit correlation functions (for $r \leq 50 h^{-1} \text{ Mpc}$) for the different redshift samples, using a fixed slope of $\gamma = 2$. ($1\text{-}\sigma$ Poisson error-bars).

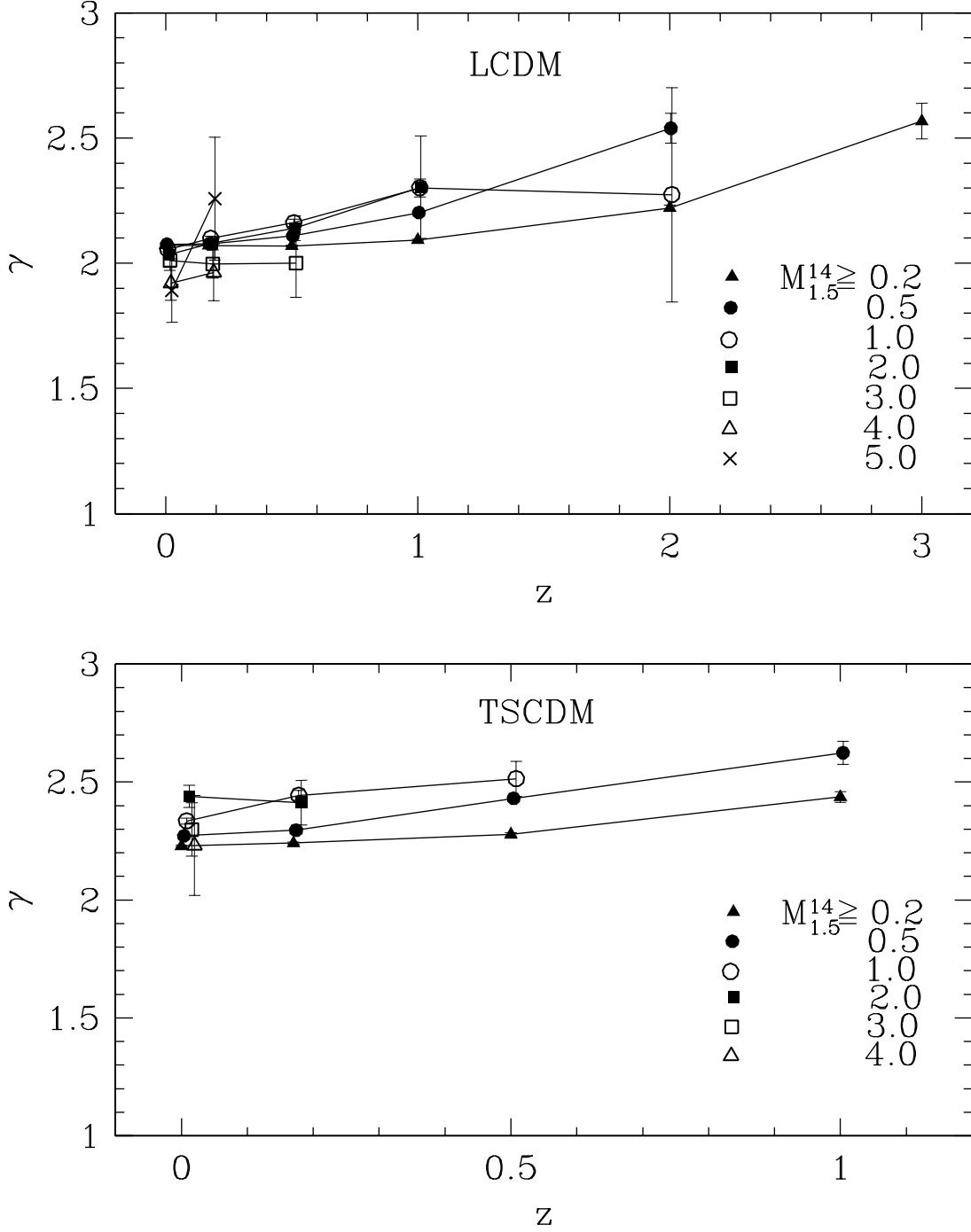


Fig. 2.— The best-fit correlation function slope (for $r \leq 50h^{-1}$ Mpc) as a function of redshift and cluster mass threshold for LCDM and TSCDM models.

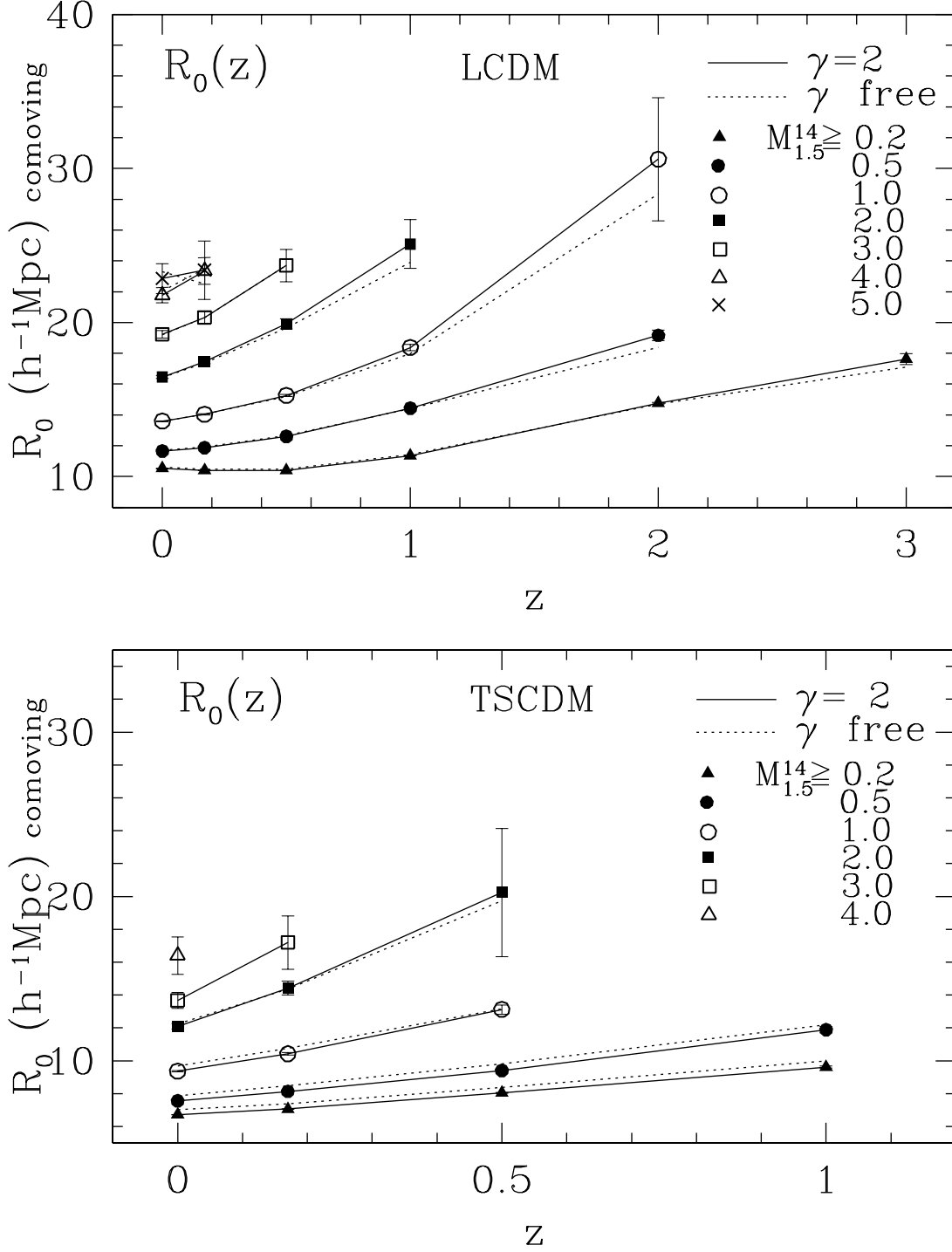


Fig. 3.— The best-fit cluster correlation scale (R_0 , comoving units) as a function of redshift and cluster mass ($M_{1.5}$). Symbols and connected solid lines are for a fixed correlation slope of $\gamma = 2$; dotted lines are for the free-fit correlation slope (Figure 2).

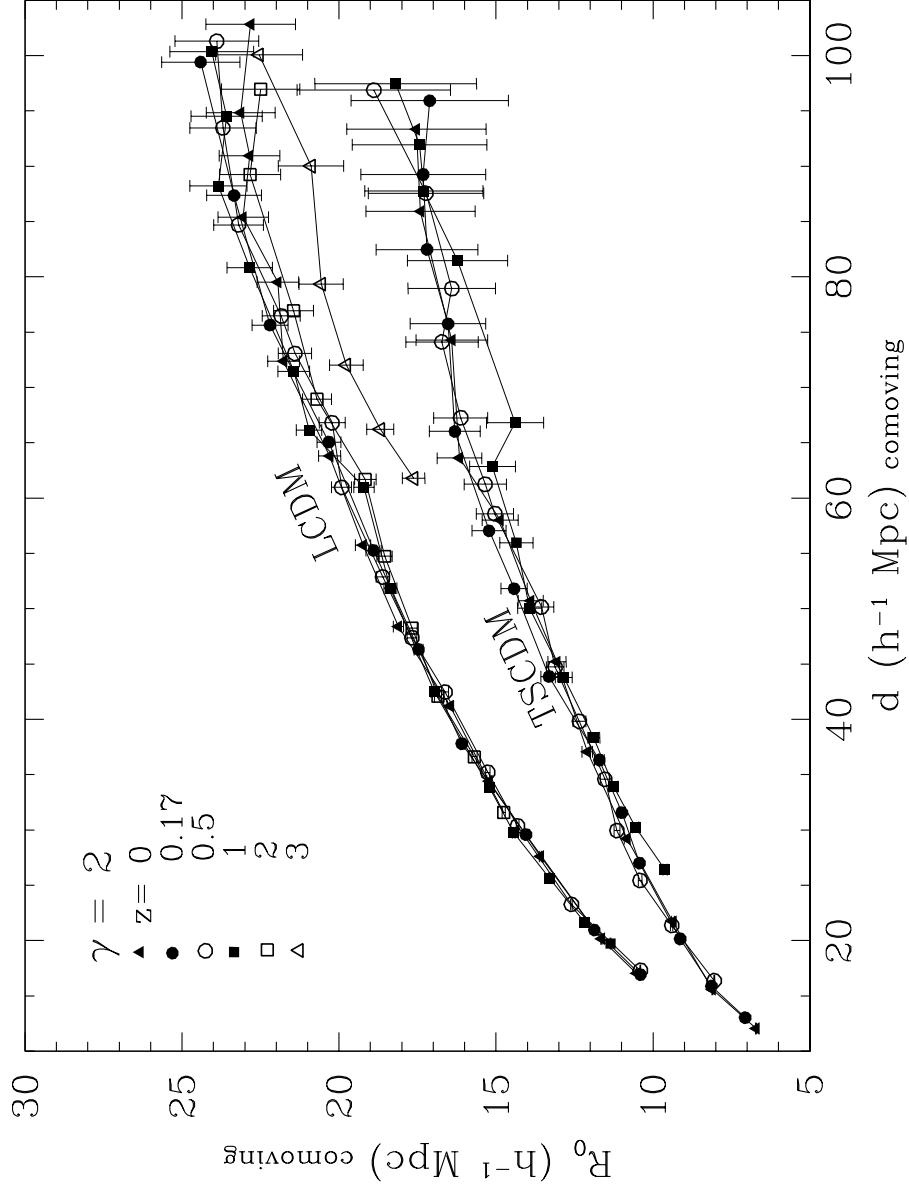


Fig. 4.— Evolution of the richness-dependent cluster correlation function, presented as the dependence of the correlation scale on the cluster mean-separation, $R_0 - d$ (comoving scales). Different symbols represent different redshifts, from $z = 0$ to $z = 3$, as indicated. The lines connect points of a given redshift. The evolution of the $R_0 - d$ relation is shown for both LCDM and TSCDM. A fixed correlation function slope of $\gamma = 2$ is used, and cluster masses are defined within a fixed comoving radius ($1.5 h^{-1} \text{ Mpc}$). (Using clusters selected instead by virial mass, which is considerably more difficult to determine observationally, produces similar results but with slightly more evolution at high d 's: the $R_0 - d$ amplitude decreases by $\lesssim 10\%$ as the redshift increases from $z = 0$ to $z = 2$ for LCDM. The R_0 amplitude is lower by $\lesssim 10\%$ at small $d \lesssim 40 h^{-1} \text{ Mpc}$ for these masses; see Section 4). $1\text{-}\sigma$ error-bars are shown.

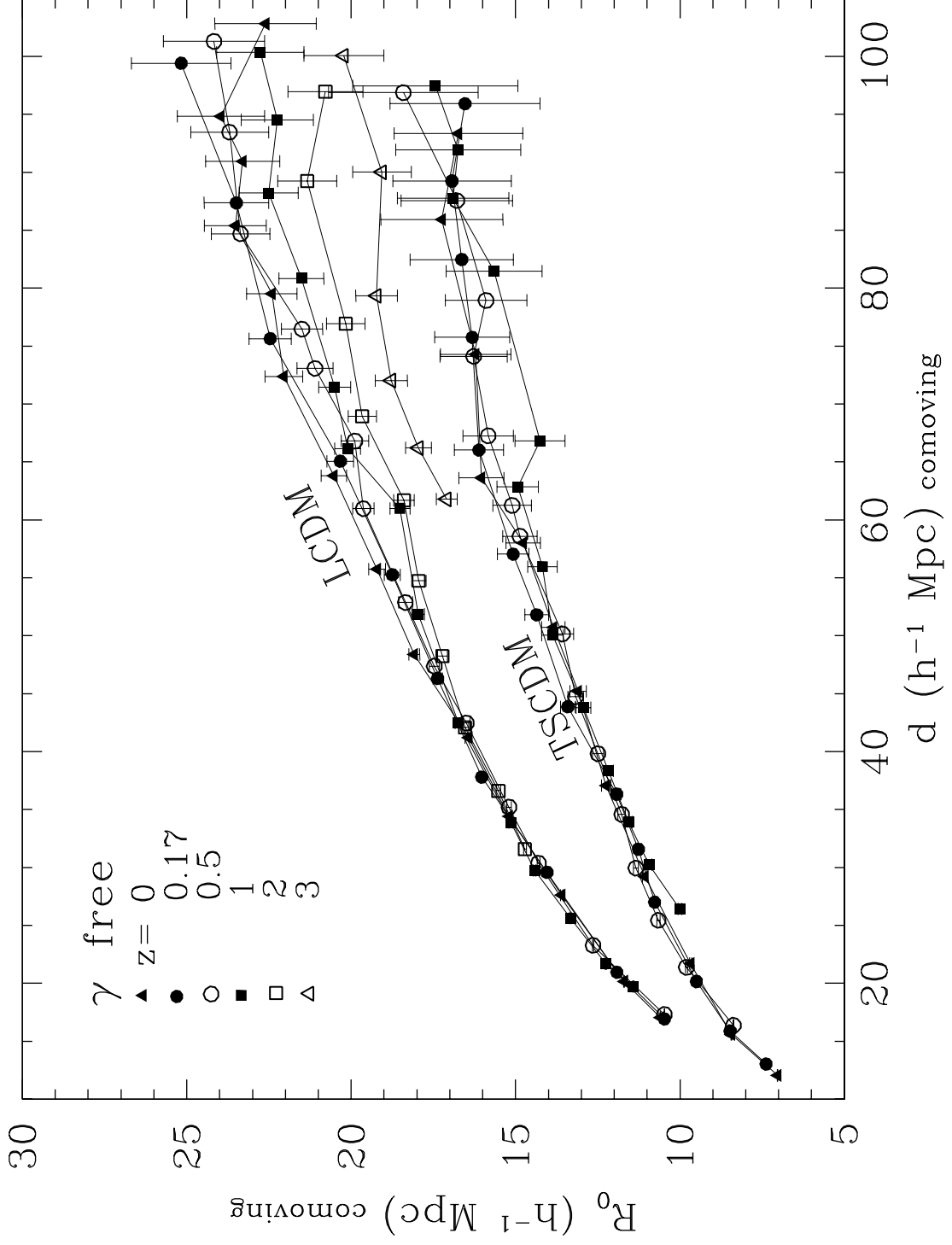


Fig. 5.— Evolution of the richness-dependent cluster correlation function. Same as Figure 4, but for a free-fit correlation function slope γ (c.f. Figures 2-3).